Structural controls on hydrothermal gold mineralization in the White River area, Yukon

Doug MacKenzie and Dave Craw
Geology Department, University of Otago[1]

MacKenzie, D.J. and Craw, D., 2010. Structural controls on hydrothermal gold mineralization in the White River area, Yukon. *In*: Yukon Exploration and Geology 2009, K.E. MacFarlane, L.H. Weston and L.R. Blackburn (eds.), Yukon Geological Survey, p. 253-263.

ABSTRACT

New mapping and drilling associated with gold exploration has elucidated the structural and lithological controls on hydrothermal gold systems in the White River area. The Paleozoic basement consists of a sequence of amphibolite facies clastic metasedimentary and meta-igneous rocks that host lower grade ultramafic rocks, some magmatically and some tectonically emplaced during the Late Triassic – Early Jurassic. Mapped ultramafic bodies show close congruence with published airborne magnetic anomalies. All of these rocks are cut by brittle normal faults and fractures, and dykes correlated with middle Cretaceous to early Tertiary extension-related intrusive rocks. Gold mineralization associated with these fractures is strongly controlled by host rock types. Two main rock types, felsic gneiss and quartzite, are preferentially fractured and hydrothermally altered. Other rock types are only weakly fractured and locally altered. In particular, ultramafic bodies and micaceous lithologies locally impeded fluid flow.

[1]*PO Box 56, Dunedin, New Zealand, doug.mackenzie@otago.ac.nz*

INTRODUCTION

The discovery of new gold-bearing hydrothermal systems in the White River area of the central western Yukon, approximately 80 km south of the Klondike goldfield (Fig. 1), has generated a new rush of exploration activity in the region. Although the geology of the area has been mapped at 1:50 000 scale (Ryan and Gordey, 2001; 2004), little is known about the gold deposits and their relationship to the surrounding rocks.

Outcrop is generally poor and limited to a few exposures on the tops of ridges and in excised streams. Most of the area is forested and zones of anomalous gold were found initially by ridge and spur soil sampling. Since the discovery of these soil anomalies in 2007, the area has been the focus of an extensive and ongoing diamond drilling program by Underworld Resources Ltd.

This report outlines results of detailed structural mapping conducted in the White River area during the 2008 and 2009 field seasons. Due to poor outcrop, field mapping was aided by published aeromagnetic data (*e.g.*, Shives *et al.*, 2002a,b) and augmented by the analysis of numerous drill core samples. This approach enabled us to determine a sequence of structural events that affected the underlying rocks and to deduce the relative timing of the gold mineralization event. We also describe the principal structural and lithological controls on mineralization. This research is part of an ongoing study supported by Underworld Resources Ltd.

REGIONAL GEOLOGY AND STRUCTURAL SETTING

The main basement lithologies in the Klondike - White River area (Fig. 1) are part of the Yukon-Tanana terrane and consist of schists and gneisses that were deformed and metamorphosed in the late Paleozoic (Mortensen, 1990, 1992, 1996; Mortensen *et al.*, 2007). The rocks range in grade from lower and upper greenschist facies in the Klondike area to amphibolite facies in the White River area. The rocks are pervasively foliated and contain at least two overprinting foliations (S_1 and S_2 of MacKenzie *et al.*, 2008a; S_T of Ryan and Gordey, 2004). The rocks were tectonically stacked along foliation-parallel thrust faults in the Early Jurassic (Mortensen, 1996) resulting in rock slices of differing metamorphic reconstitution being juxtaposed (MacKenzie *et al.*, 2008b). Slices of Triassic metasedimentary rocks and mafic and ultramafic rocks of the Slide Mountain terrane (Mortensen, 1990, 1996) were incorporated into the thrust stack at this time. The regional-scale thrust faults are generally poorly exposed but are locally marked by lenses of sheared ultramafic rocks and serpentinite. Thrust imbrication resulted in local macroscopic semi-ductile folding and shearing, and the development of a crenulation cleavage in the rocks adjacent to thrusts. All of these metamorphic and thrust-related fabrics were then locally overprinted by m-scale semibrittle upright folds and associated angular kink folds and fractures (MacKenzie *et al.*, 2008a). By the mid-Cretaceous these compressional features were cut by post-metamorphic extensional structures that accompanied exhumation of the metamorphic pile. Felsic and mafic igneous rocks were intruded at this time, their emplacement controlled by coeval normal faults (Gabrielse and Yorath, 1991; Mortensen, 1996). Regional extension continued through the Cretaceous to the Eocene, when initiation of the Tintina fault (Fig. 1) resulted in ~450 km of strike-slip displacement (Gabrielse *et al.*, 2006). Minor regional uplift continued until the late Tertiary and erosion of basement led to concentration of gold-bearing gravels into numerous district-wide alluvial placer deposits (*e.g.,* Lowey, 2006; LeBarge, 2007).

STRUCTURAL GEOLOGY

The basement rocks of the White River area (Figs. 1, 2) consist of an interlayered sequence (1-100 m) of amphibolite-facies quartzite, marble, hornblende gneiss, biotite gneiss (locally garnet-bearing) and felsic gneiss (locally containing millimetre to centimetre-scale K-feldspar augen). All of these lithologies contain a pervasive foliation (S_2) that is a composite feature, composed of at least one earlier metamorphic foliation (S_1) that was folded and reactivated by a second phase of ductile deformation during peak metamorphism (D_2; Table 1). This S_2 foliation is generally shallowly to moderately NE-dipping (30° to 50°) over most of the study area, except where locally steepened by later deformation (D_3-D_5; Table 1).

The most prominent folds in the area are m-scale, late metamorphic, tight to isoclinal folds (Fig. 2b) that are best developed in and near semiductile deformation zones (D_3; Table 1). The axial planes of these folds (F_3) are generally shallowly dipping and subparallel to the regional S_2 foliation (Fig. 3a). Where D_3 deformation is most intense, crenulation cleavage, semi-ductile shears, fractures and breccia zones developed parallel to fold axial surfaces (Fig. 3b). Serpentinite bodies (1-50 m thick) are commonly associated with zones of strong D_3

deformation. Here they are tightly folded, sheared and metasomatically altered to greenschist facies minerals (e.g., chlorite, talc, actinolite; Fig. 4). Where folding has been intense, the hinges of tight F_3 crenulations define a new closely spaced S_3 fold-axial-surface cleavage (Fig. 4a,c,d). The serpentinites are commonly magnetic and locally contain up to 1-2% euhedral magnetite. Lensoid bodies of serpentinite form prominent magnetic highs and stand out from the surrounding gneiss sequence in aeromagnetic images (Fig. 5a). Some of the serpentinite bodies form lenses that pinch in and out along zones of strong F_3 folding and interpreted thrust faults (Fig. 5b).

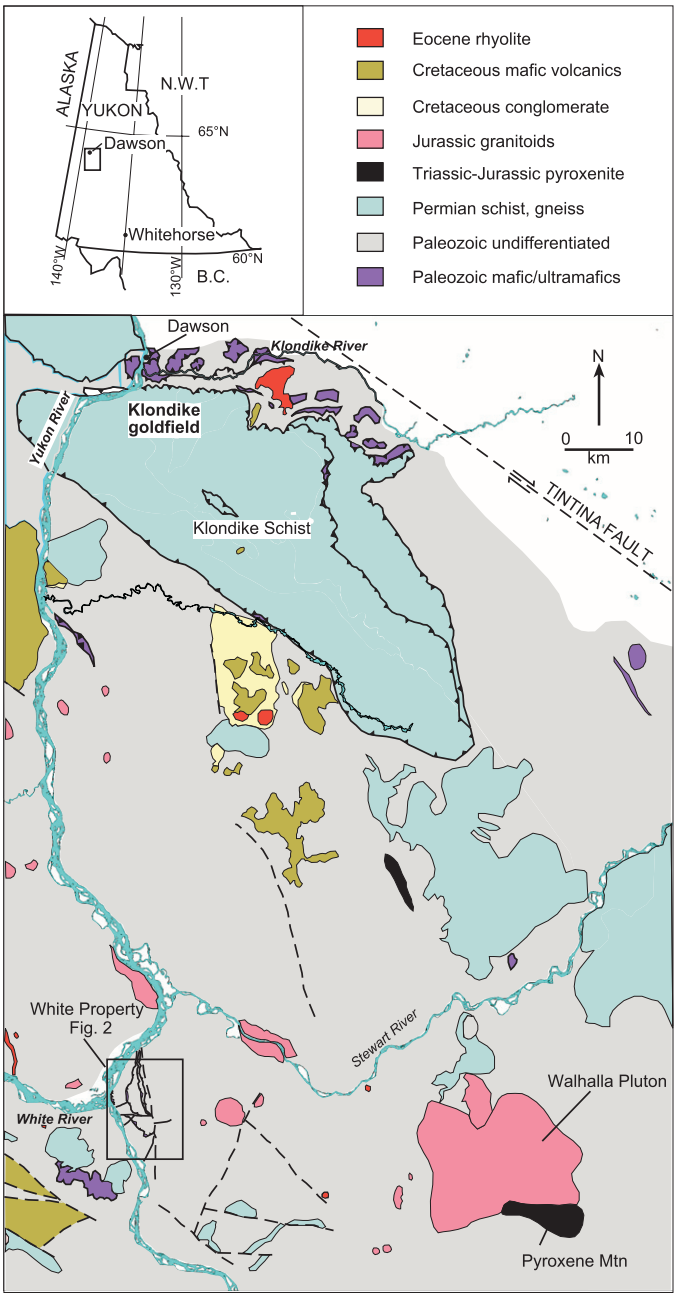

Figure 1. *Geological map of the Klondike - White River area (modified after Ryan and Gordey, 2004 and MacKenzie et al., 2008a). Top inset map outlines the study area within the Yukon. The location of the White Property and Figure 2 are indicated lower left.*

A bimodal suite of pyroxenite and light-coloured felsic granitoid dykes and sills (1-20 m thick) intrude the gneiss sequence (Fig. 6a). These bodies are relatively massive, coarse-grained (pyroxenites locally contain cm-scale pyroxene crystals) and lack the S_2 metamorphic foliation. They are locally affected by D_3 structures, and in strong D_3 deformation zones, pyroxenite bodies form massive pods that are cut by shears and a new greenschist facies S_3 foliation, especially along their margins (Fig. 3c, 6b). These dykes and sills are petrogaphically similar to larger Late Triassic – Early Jurassic pyroxenite and granitoid intrusions that crop out 40-50 km east (e.g., Pyroxene Mountain and Walhalla Plutons; Fig. 1; J.K. Mortensen, unpublished data; Gordey and Ryan, 2005). Although they do not contain visible magnetite like the serpentinite rocks, the pyroxenite bodies are also coincident with prominent magnetic highs in the aeromagnetic images (Fig. 5a).

The D_3 structures are locally overprinted by rare semi-brittle folds, angular kinks and fractures (D_4; Table 1). F_4 folds and kinks are typically upright, at high angle to the S_2 foliation and have an associated axial surface fracture. These D_4 structures are weakly developed in the White River area (*c.f.*, MacKenzie *et al.*, 2007, 2008a); outcrops that show evidence for this phase of deformation are generally only sporadically distributed throughout the region.

The basement gneiss sequence and post-metamorphic ultramafic and felsic rocks are cut by a set of high-angle north and east-striking normal faults (Figs. 2a,b). These faults represent the youngest recognized deformation event in the White River area (D_5; Table 1) and cut across all earlier structures. The faults are generally poorly exposed in outcrop, but where intersected in drill core, they juxtapose different lithologic units in the gneiss sequence. The F_5 faults and fracture zones locally host felsic aphanitic dykes that are correlated with mid-Cretaceous to early Tertiary extension-related igneous activity (Gabrielse and Yorath, 1991; Mortensen, 1996). Several Mesozoic granitoid plutons (up to 2 km in diameter) crop out approximately 10 km east of the White River area (Fig. 1; Ryan and Gordey, 2001).

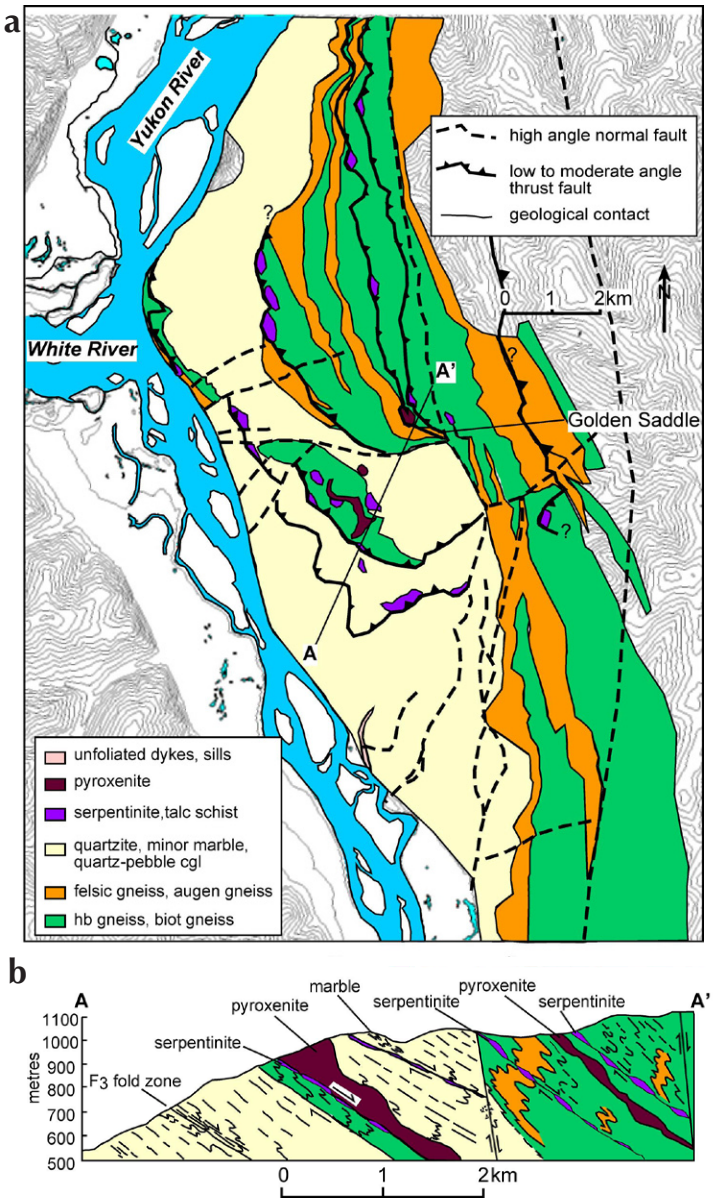

Figure 2. *Geology of the White River area.* ***(a)*** *Geological map based in part on Ryan and Gordey (2004) and on detailed field mapping conducted by the authors and Underworld Resources personnel.* ***(b)*** *Northeast cross section through Golden Saddle (line A-A') showing the structural relationships between gneisses and post-metamorphic ultramafic bodies. cgl = conglomerate, hb = hornblende, biot = biotite.*

Table 1. *Summary of principal structural events relevant to gold mineralization in the White River area (modified after Berman et al., 2007).*

Regional structural event	Structures	Alteration/ mineralization	Age
D_5	Steeply dipping normal faults, felsic dykes (m-scale)	Hydrothermal alteration and disseminated gold mineralization controlled by lithologic layering and steeply dipping fractures	Middle Cretaceous-early Tertiary
D_4	Rare angular kink folds and upright warps; local veins along fold axial surfaces	Massive mm to m-scale white quartz veins controlled by fold axial surface fractures	Jurassic
D_3	Ductile folds, shears and chloritic foliation, especially associated with ultramafic horizons and thrusts	Greenschist facies retrogression, mainly subparallel to S_2	Jurassic
Bimodal pyroxenite and granitoid intrusion	Dykes and sills intruded into D_3 deformation zones		Late Triassic-Early Jurassic
D_2	Pervasive amphibolite facies foliation (S_2), stretching lineation, rare isoclinal folds (F_2)		Late Paleozoic
D_1	rare S_1 segregations preserved in intrafolial fold hinges, almost completely transposed by D_2		Late Paleozoic

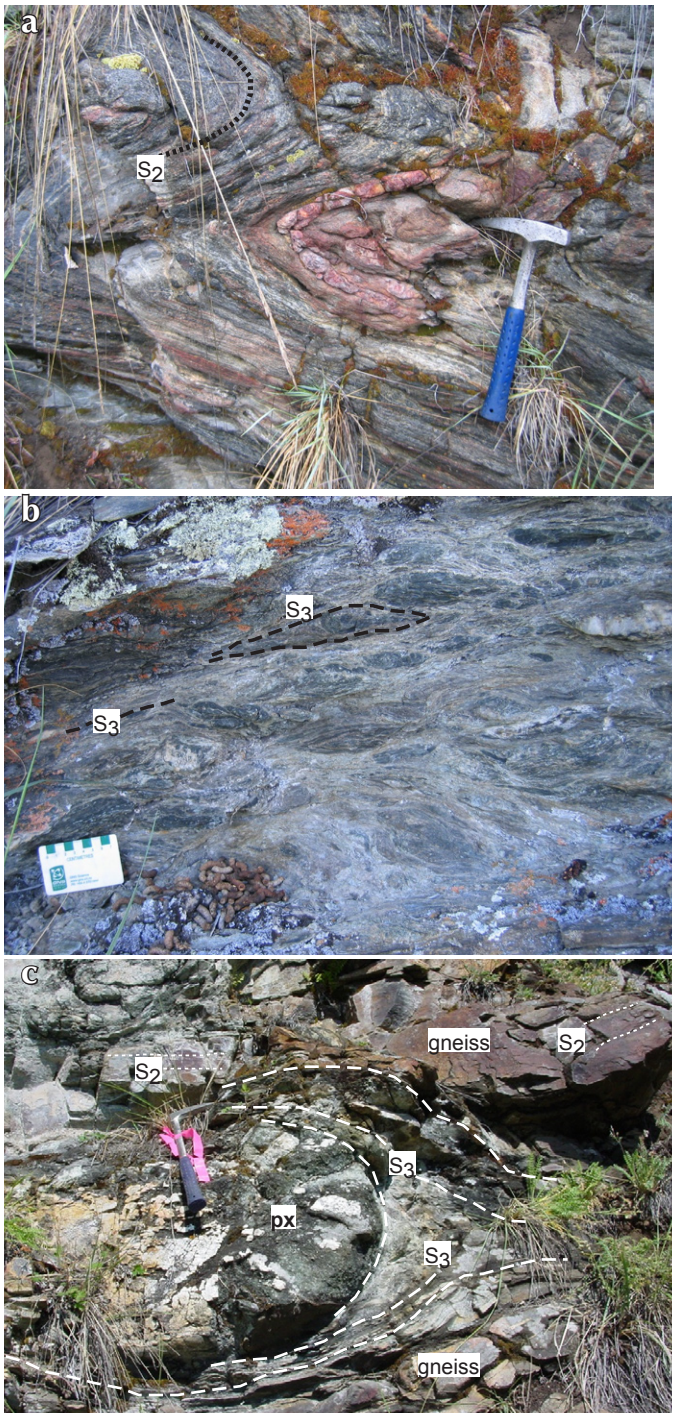

Figure 3. *F_3 folds, ductile shears and S_3 foliation.* ***(a)*** *Outcrop of strongly folded biotite gneiss. Prominent S_2 foliation (black dashed line) is highly folded by F_3 folds.* ***(b)*** *Zone of ductile shearing in biotite gneiss. S_3 foliation (dashed lines) anastomoses around lenses of sheared gneiss.* ***(c)*** *S_3 foliation (long-dashed lines) cuts through an outcrop of biotite gneiss at an angle to S_2 (short-dashed lines) and anastomoses around a relatively massive pod of pyroxenite (px).*

MINERALIZATION

Hydrothermal fluid flow and gold mineralization is controlled primarily by brittle normal faults that cut the metamorphic structures. However, there has been little emplacement of auriferous quartz veins along these faults and most of the gold occurs in altered rocks adjacent to the faults. Fluid penetration into the rock mass adjacent to the faults is controlled by fractures in brittle host rocks, especially brecciated zones (Fig. 7). These features are generally steeply dipping, subparallel to the normal faults. In addition, shears and foliation associated with F_3 folding facilitated penetration of fluids parallel to S_3, which is typically shallow-dipping subparallel to S_2 (Fig. 2).

Hydrothermal alteration mineralogy is strongly controlled by host rock mineralogy. Felsic gneisses have an oxidized alteration assemblage, with abundant hematite and sericite (Fig. 7a-d). Hematite is most prominent in weakly altered rocks (Fig. 7b), and strongly altered rocks have hematite replaced by pyrite (Fig. 7c,d). Gold occurs in, and is closely associated with pyrite, and the highest gold grades occur in pyritic breccias (Fig. 7d). Quartzites have a reduced metamorphic assemblage, with accessory graphite and pyrrhotite (Fig. 7e). Hence, hydrothermal alteration is also reduced in these rocks and is dominated by recrystallization of graphite and pyrrhotite, with localized addition of arsenopyrite (Fig. 7f,g,h). Gold is enriched in arsenopyrite-bearing rocks, including those with stylolitic seams (Fig. 7f,g) and breccias (Fig. 7h). Late-stage pharmacosiderite (K-Fe-arsenate) occurs locally within mineralized rocks.

Biotite and hornblende gneisses, pyroxenites, and serpentinite horizons have deformed in more ductile manner than felsic gneisses and quartzites during normal faulting. Hence, fracture networks are poorly developed in these rock types and there has been little hydrothermal alteration and addition of gold. Pyroxenites have locally altered to fuchsite (Fig. 6c), and serpentinite bodies have non-penetrative fuchsite-talc-carbonate alteration (Fig. 4d). Both these ultramafic alteration processes involved formation of rutile and pyrite from pre-existing metallic minerals, and magnetite has decomposed. Hence, the minor hydrothermal alteration has decreased the magnetic signature of the ultramafic bodies that otherwise makes them mappable regionally (Fig. 5).

Figure 4. *Altered serpentinite and biotite gneiss in drill core.* ***(a)*** *Contact between dark grey biotite gneiss and light green chlorite-altered serpentinite and talc-carbonate schist. S_2 foliations in biotite gneiss exhibit ductile folds from F_3 folding. Serpentinite and talc-carbonate schist are strongly crenulated.* ***(b)*** *Close-up of garnetiferous biotite schist with relatively planar S_2 foliation defined by green and black micaceous minerals (running top right to bottom left).* ***(c)*** *Close-up of talc carbonate schist (white) and chlorite (green). Crenulations in micaceous fabric define weak S_3 foliation.* ***(d)*** *Fuchsite-altered serpentinite with F_3 crenulations.*

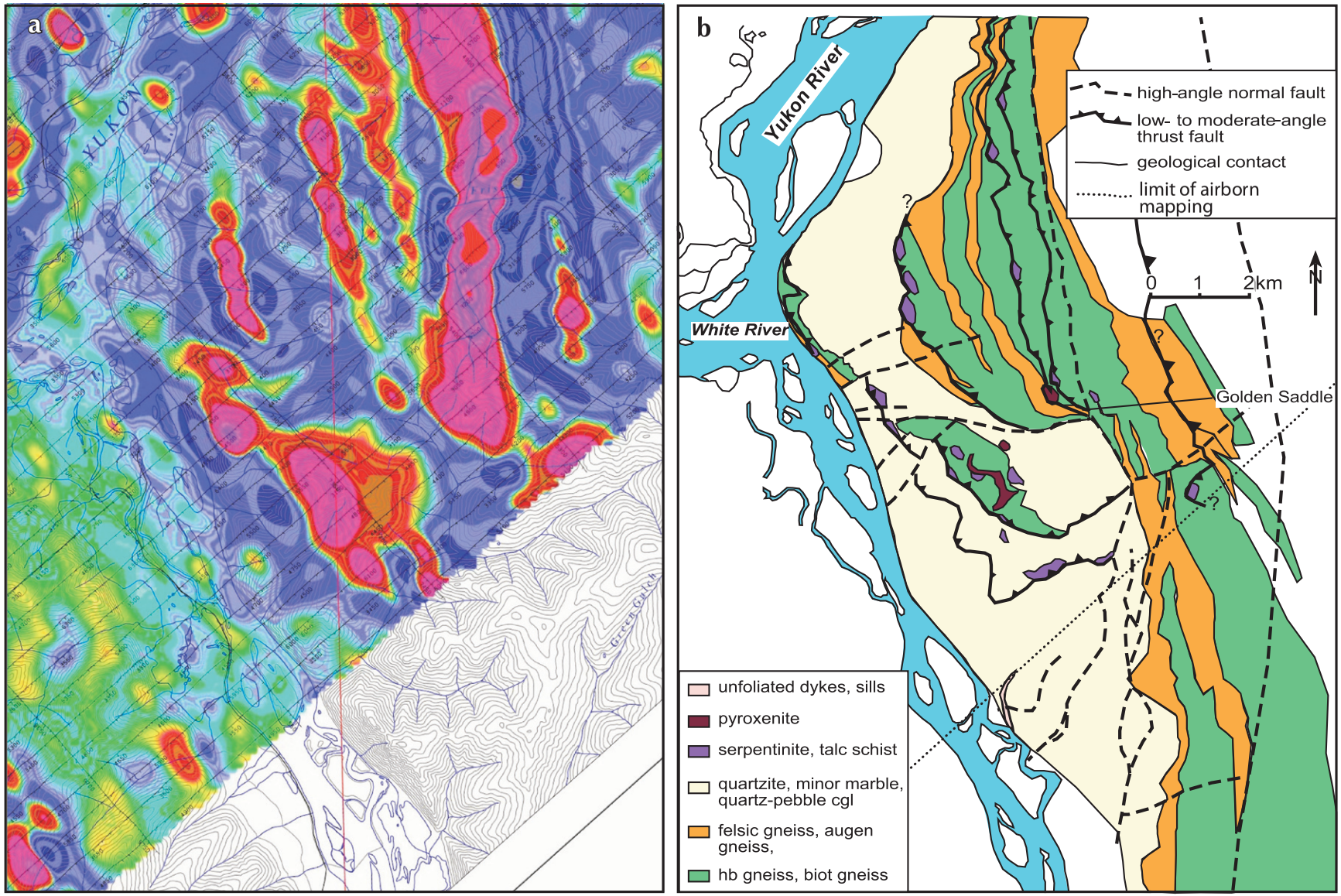

Figure 5. *Comparison of airborne magnetic response with mapped geology in the White River area.* ***(a)*** *Magnetic first vertical derivative map (after Shives et al., 2002b). Magnetic highs (red, yellow, orange) show close congruence with mapped ultramafic bodies.* ***(b)*** *Geological map of the White River area as in Figure 1.*

Figure 6. *Pyroxenite intrusions.* ***(a)*** *Dark green coarse-grained pyroxenite (mm to cm-scale pyroxene crystals) and associated felsic veining (white) contains blocky inclusions of light grey biotite gneiss (left of centre).* ***(b)*** *Relatively massive pyroxenite and associated felsic veins (white) cut by S_3 foliation (white dashed line) on upper margin.* ***(c)*** *Boundary between altered fuchsite-bearing pyroxenite (light green) and unaltered pyroxenite (dark green) in drill core.*

Figure 7. *(next page) Drill core from Golden Saddle, showing the two main rock types that are fractured and altered in the White River area.* ***(a)*** *Felsic gneiss with prominent S_2 foliation defined by black biotite (running top to bottom) anastomosing around relict K- feldspar augen (white).* ***(b)*** *Weakly altered felsic gneiss with red hematite and yellow sericite alteration. Fine hydrothermal pyrite is disseminated in the alteration patches. White bleaching defines fracture-controlled silicification.* ***(c)*** *Highly fractured, sericitised (yellow) and silicified (white) felsic schist. Dark grey pyrite veins infill fractures.* ***(d)*** *Strongly silicified and sericitized felsic gneiss breccia infilled with quartz and pyrite.* ***(e)*** *Quartzite with prominent S_2 foliation defined by fine graphitic laminations (running top left to bottom right) cut by numerous brittle fractures and quartz veins.* ***(f)*** *Folded quartzite with S_2 foliation, defined by graphitic laminations, cut by dark stylolites and shears containing hydrothermal graphite and local arsenopyrite.* ***(g)*** *Quartzite with S_2 foliation almost completely disrupted by fractures, shears and incipient stylolite development.* ***(h)*** *Strongly silicified quartzite and quartz vein breccia infilled with quartz, pyrite and arsenopyrite.*

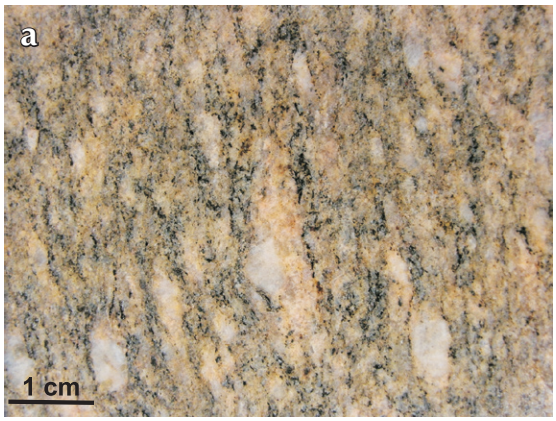
a
1 cm

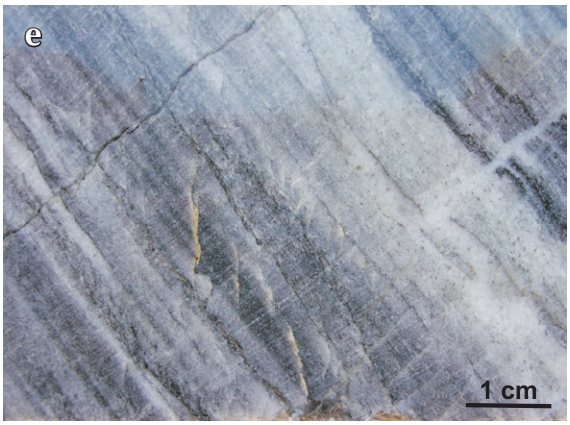
e
1 cm

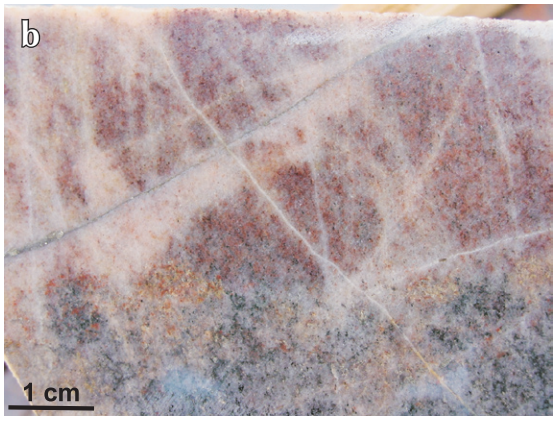
b
1 cm

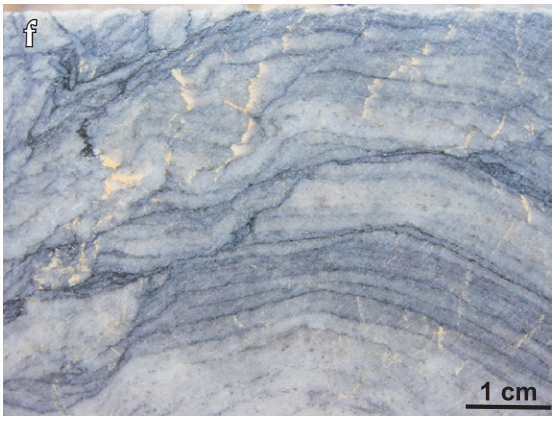
f
1 cm

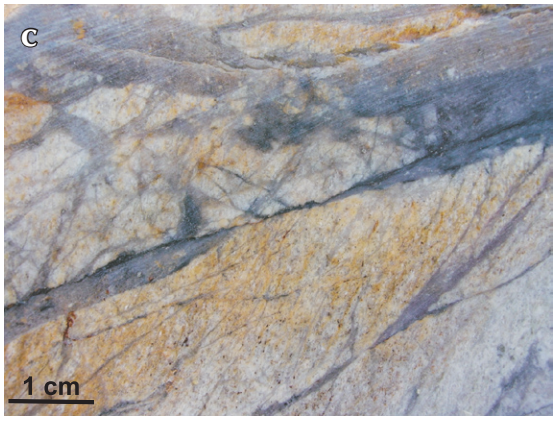
c
1 cm

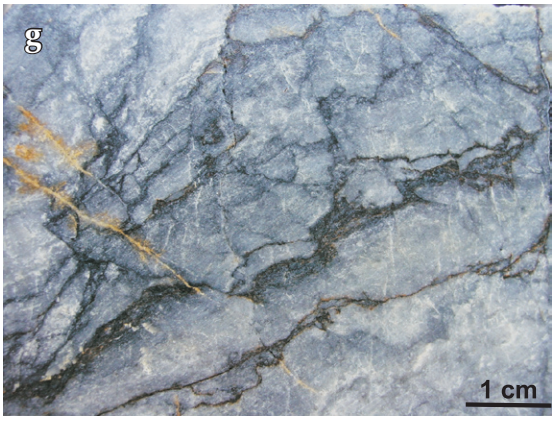
g
1 cm

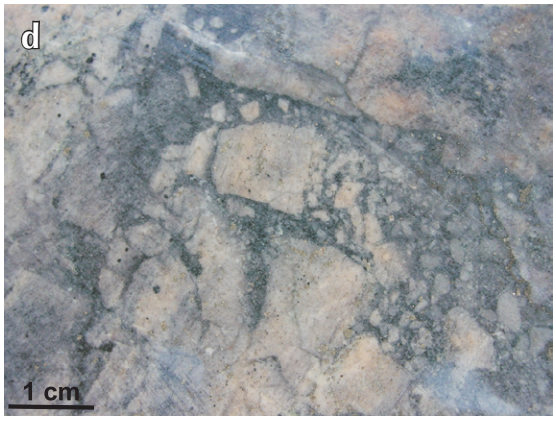
d
1 cm

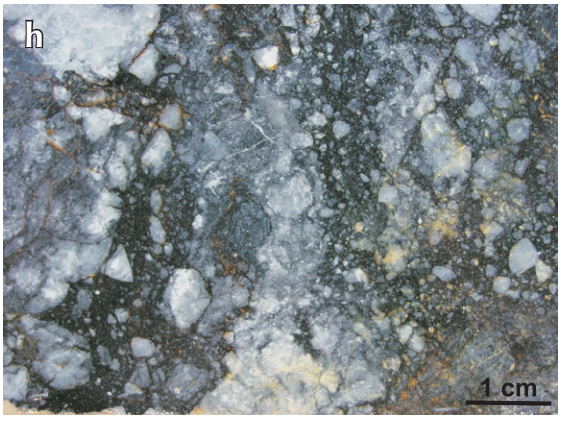
h
1 cm

DISCUSSION AND CONCLUSIONS

Two distinctly different types of ultramafic bodies have been emplaced into the amphibolite facies gneissic sequence in the White River area, and their magnetic signatures have been helpful for mapping the area. Sill-like pyroxenite bodies were intruded subparallel to the regional pervasive metamorphic foliation, and these bodies have been deformed by a localized greenschist facies foliation associated with tight recumbent folding and thrusting of that foliation. Serpentinite bodies have been emplaced by thrust faults into the gneisses, and these serpentinite bodies have also been affected by the greenschist facies fabric that formed in association with the thrust faults.

The gneissic rock mass and emplaced ultramafic bodies have been cut by moderately to steeply dipping brittle normal faults with northerly and easterly strikes. These faults formed in the Late Cretaceous or early Tertiary. The normal faults have disrupted the gneisses into structural blocks on the km-scale, and have juxtaposed distinctly different rock types. This disruption of rock types can be mapped in a general way using magnetic signatures of the enclosed ultramafic rocks.

The normal faults have acted as conduits for hydrothermal fluids that introduced gold to the White River area. There was little emplacement of quartz veins during this hydrothermal activity, and most mineralization is disseminated through the gneisses adjacent to the faults. Fluid flow was controlled by brittle fractures and breccias associated with the faults, and also by shallow-dipping shears associated with the greenschist facies folds and thrust faults.

Hydrothermal alteration was strongly controlled by rock types adjacent to the normal faults. Felsic gneisses and quartzites have the best-developed fracture systems, and are the principal hosts for introduced gold. Felsic gneisses have an oxidised alteration assemblage dominated by hematite and sericite, with later stage pyritic alteration that contains the highest gold grades. In contrast, quartzites, with metamorphic graphite and pyrrhotite, have a reduced alteration assemblage with recrystallized graphite and pyrrhotite and introduced arsenopyrite. Gold grades are highest in arsenic-rich rocks in quartzites. Other gneisses and the ultramafic rocks have had only limited hydrothermal interaction because of lack of fracturing, and gold addition has been minimal. Ultramafic rocks have localised fuchsitic alteration and associated decomposition of primary magnetite. Magnetite decomposition affects the geophysical signature of these rocks, and this may be visible in detailed magnetic surveys.

ACKNOWLEDGEMENTS

Financial assistance for this research was provided by Underworld Resources Ltd., the University of Otago, and the NZ Foundation for Research, Science and Technology. Discussions with Adrian Fleming, Rob McLeod, Mike Cooley, Lamont Leatherman, Colin Brodie, Jodie Gibson and Hanne-Kristen Paulsen helped us to develop our ideas. The map in Figure 2 incorporates some aspects of an unpublished map by Chris Ash for Madalena Ventures Inc. 2005. A constructive review by Jim Mortensen helped improve the manuscript.

REFERENCES

Berman, R.G., Ryan, J.J., Gordey, S.P. and Villeneuve, M. 2007. Permian to Cretaceous polymetamorphic evolution of the Stewart River region, Yukon-Tanana terrane, Yukon, Canada: P-T evolution linked with *in situ* SHRIMP monazite geochronology. Journal of Metamorphic Geology, vol. 25, p. 803-827.

Gabrielse, H. and Yorath, C.J., 1991. Tectonic synthesis, Chapter 18. *In:* Geology of the Cordilleran Orogen in Canada, H. Gabrielse and C.J. Yorath (eds.), Geological Survey of Canada, Geology of Canada, vol. 4, p. 677-705. (also Geological Society of America, The Geology of North America, v. G-2)

Gabrielse, H., Murphy, D.C. and Mortensen, J.K., 2006. Cretaceous and Cenozoic dextral orogen-parallel displacements, magmatism, and paleogeography, north-central Canadian Cordillera. *In:* Paleogeography of the North American Cordillera: Evidence For and Against Large-Scale Displacements, J.W. Haggart, R.J. Enkin and J.W.H Monger (eds.), Geological Association of Canada, Special Paper 46, p. 255-276.

Gordey, S.P. and Ryan, J.J., 2005. Geology map, Stewart River Area (115 N, 115–O and part of 115J), Yukon Territory. Geological Survey of Canada, Open File 4970, 1:250 000 scale.

LeBarge, W.P., 2007. Yukon Placer Mining Industry, 2003-2006: An overview of placer activity and production. *In:* Yukon Placer Mining Industry 2003-2006, W.P. LeBarge and C.S. Welsh (compilers), Yukon Geological Survey, 235 p.

Lowey, G.W., 2006. The origin and evolution of the Klondike goldfields, Yukon, Canada. Ore Geology Reviews, vol. 28, p. 431-450.

MacKenzie, D.J., Craw, D.C., Mortensen, J.K. and Liverton, T., 2007. Structure of schist in the vicinity of the Klondike goldfield, Yukon. *In:* Yukon Exploration and Geology 2006, D.S. Emond, L.L. Lewis and L.H. Weston (eds.), Yukon Geological Survey, p. 197-212.

MacKenzie, D.J., Craw, D. and Mortensen, J., 2008a. Structural controls on orogenic gold mineralization in the Klondike goldfield, Canada. Mineralium Deposita, vol. 43, p. 435-448.

MacKenzie, D., Craw, D. and Mortensen, J.K., 2008b. Thrust slices and associated deformation in the Klondike goldfields, Yukon. *In:* Yukon Exploration and Geology 2007, D.S. Emond, L.R. Blackburn, R.P. Hill and L.H. Weston (eds.), Yukon Geological Survey, p. 199-213.

Mortensen, J.K., 1990. Geology and U-Pb chronology of the Klondike District, west-central Yukon. Canadian Journal of Earth Sciences, vol. 27, p. 903-914.

Mortensen J.K., 1992. Pre-mid-Mesozoic tectonic evolution of the Yukon-Tanana Terrane, Yukon and Alaska. Tectonics, vol. 11, p. 836-853.

Mortensen, J.K., 1996. Geological compilation maps of the northern Stewart River map area, Klondike and Sixtymile Districts (115N/15, 16; 1150/13, 14; and parts of 1150/15, 16). Exploration and Geological Services Division, Yukon Region, Indian and Northern Affairs Canada, Open File 1996-1(G), 43 p.

Mortensen, J.K., Beranek, L. and Murphy, D.C., 2007. Permo-Triassic Orogeny in the Northern Cordillera: Sonoma North? Geological Society of America, Abstracts with Programs, 103rd Annual Meeting, Cordilleran Section, Bellingham, WA, USA, Paper No. 28-5.

Ryan, J.J. and Gordey, S.P., 2001. Geology of the Thistle Creek area, Yukon Territory (115-O/3). Geological Survey of Canada, Open File 3690, 1:50 000 scale.

Ryan, J.J. and Gordey, S.P., 2004. Geology, Stewart River Area (Parts of 115 N/1,2,7,8 and 115–O/2-12), Yukon Territory. Geological Survey of Canada, Open File 4641, 1:100 000 scale.

Shives, R.B.K., Carson, J.M., Ford, K.L., Holman, P.B., Gordey, S. and Abbott, G., 2002a. Magnetic Anomaly Map (Residual Total Field), Stewart River Area – 115O/6, 1:50 000 scale. Geological Survey of Canada, Open File 4307; Exploration and Geological Services Division, Yukon, Indian and Northern Affairs Canada, Open File 2002-13.

Shives, R.B.K., Carson, J.M., Ford, K.L., Holman, P.B., Gordey, S. and Abbott, G., 2002b. Magnetic First Vertical Derivative Map Stewart River Area – 115O/6, 1:50 000 scale. Geological Survey of Canada, Open File 4307; Exploration and Geological Services Division, Yukon, Indian and Northern Affairs Canada, Open File 2002-13.